CONTOUR EXTRACTION IN PROSTATE ULTRASOUND IMAGES USING THE WAVELET TRANSFORM AND SNAKES

Fangwei Zhao† and Christopher J.S. deSilva†‡
†Centre for Intelligent Information Processing Systems
‡Australian Research Centre for Medical Engineering
The University of Western Australia, Crawley WA 6009, AUSTRALIA
email: zhao@ee.uwa.edu.au, chris@ee.uwa.edu.au

Abstract—**It is extremely difficult to locate the contour of the prostate in B-scan ultrasound images automatically by computer because of low resolution and high noise levels. In this paper we present a semi-automatic prostate contour extration scheme, which is based on the wavelet transform and active contour models, or snakes. The ultrasound image is first decomposed into edge maps at different resolutions via the wavelet transform. Seed points are found in the coarsest edge map by examining the maxima along the radial profiles which emanate from an anchor point selected manually. These seed points are used to initialize a snake, which will evolve across the edge maps at different resolutions and eventually converge to the contour of the prostate.**

Keywords—**Ultrasound, prostate, wavelet, edge detection, active contour models, snakes, deformable models**

I. Introduction

Prostate cancer has become a focus of new interest as the population ages and the death rate due to cardiovascular disease decreases. Advanced prostate cancer is not curable, but when it is diagnosed in an early stage, it is curable [1], [2]. This prompts the need to improve the detection rate of the disease in early diagnosis.

Accurate detection of prostate contours is essential to many diagnostic and treatment procedures. For example, prostate-specific antigen density (PSAD) is very useful in differentiating benign from malignant prostate disease. PSAD involves the estimation of the prostate gland volume, which is derived from the boundaries. Contour information is also helpful in directing biopsy needles to the suspicious site and monitoring volume change of hypoechoic lesions. Currently the boundaries of the prostate are manually outlined by a urologist, which is a tedious and challenging task. Moreover, inter-observer and intra-observer variability is inevitable. So automatic contour extraction by computer would be of great value.

Unfortunately it is extremely difficult to determine the prostate boundaries automatically by computer due to the low resolution and poor contrast of B-scan ultrasound images, accompanied by the high level of speckle noise due to scattering and other complicated interactions between ultrasonic pulses and human tissue. Moreover, missing boundary segments are not uncommon, which are attributed to acoustic shadowing, and/or hyperechoic structures within or around the prostate gland.

As an earlier attempt, a contour detection scheme using the Laplacian of Gaussian filter was applied[3]. The problem with this scheme was that it is difficult to find a proper threshold. Too many or too few edges may be found depending on the threshold selected, which makes it difficult to track all the relevant edges that correspond to the object and form a closed contour from these boundary segments.

Our novel contour extraction scheme consists of the following steps: first the ultrasound image is decomposed into edge maps at different resolutions using the wavelet transform. Then some seed points are found in the coarsest edge map. A snake is initialised using these seed points, which evolves across the edge maps at different scales and finally converges to the contour of the prostate.

II. Contour Extraction Scheme

A. Multiscale Edge Detection

Wavelets are families of scaled and shifted versions of a mother wavelet, which is usually a waveform of limited duration with an average value of zero. One major advantage offered by wavelet analysis is its ability to perform local analysis, that is, the wavelets' localized support means that some local features, such as abrupt transitions of a signal, can be better depicted or revealed by wavelets than by other means.

The quadratic spline wavelet and its scaling function of relevance to the discrete wavelet transform that follows were first introduced by Mallat and Zhong [4]. The quadratic spline wavelet is the first order derivative of its scaling function, which closely approximates a Gaussian function. The wavelet decomposition of an image $I(x,y) \in \boldsymbol{L}^2(\boldsymbol{R}^2)$ at scale 2^j has two components, $d^H_{2^j}(x,y)$ and $d^V_{2^j}(x,y)$, defined by the convolution with the two directional wavelets $\psi^H_{2^j}(x,y)$ and $\psi^V_{2^j}(x,y)$ respectively

$$\begin{aligned} d^H_{2^j}(x,y) &= \psi^H_{2^j}(x,y) * I(x,y) \\ d^V_{2^j}(x,y) &= \psi^V_{2^j}(x,y) * I(x,y) \end{aligned} \quad (1)$$

The two directional wavelets are given by the partial

Report Documentation Page

Report Date	Report Type	Dates Covered (from... to)
25 Oct 2001	N/A	-

Title and Subtitle Contour Extraction in Prostate Ultrasound Images Using the Wavelet Transform and Snakes	**Contract Number**
	Grant Number
	Program Element Number
Author(s)	**Project Number**
	Task Number
	Work Unit Number
Performing Organization Name(s) and Address(es) Centre for Intelligent Information Processing Systems Australia	**Performing Organization Report Number**
Sponsoring/Monitoring Agency Name(s) and Address(es) US Army Research, Development & Standardization Group (UK) PSC 802 Box 15 FPO AE 09499-1500	**Sponsor/Monitor's Acronym(s)**
	Sponsor/Monitor's Report Number(s)

Distribution/Availability Statement
Approved for public release, distribution unlimited

Supplementary Notes
Papers from 23rd Annual International Conference of the IEEE Engineering in Medicine and Biology Society, October 25-28, 2001, held in Istanbul, Turkey. See also ADM001351 for entire conference on cd-rom. , The original document contains color images.

Abstract

Subject Terms

Report Classification unclassified	**Classification of this page** unclassified
Classification of Abstract unclassified	**Limitation of Abstract** UU

Number of Pages
4

derivative of the corresponding spline scaling function $\phi_{2^j}(x,y)$ as follows

$$\begin{aligned} \psi^H_{2^j} &= \frac{\partial \phi_{2^j}(x,y)}{\partial x} \\ \psi^V_{2^j} &= \frac{\partial \phi_{2^j}(x,y)}{\partial y} \end{aligned} \tag{2}$$

By substituting (2) into (1) we get

$$\begin{aligned} \begin{pmatrix} d^H_{2^j}(x,y) \\ d^V_{2^j}(x,y) \end{pmatrix} &= \begin{pmatrix} \psi^H_{2^j}(x,y) * I(x,y) \\ \psi^V_{2^j}(x,y) * I(x,y) \end{pmatrix} \\ &= \begin{pmatrix} \frac{\partial}{\partial x}(\phi_{2^j} * I)(x,y) \\ \frac{\partial}{\partial y}(\phi_{2^j} * I)(x,y) \end{pmatrix} \\ &= \nabla(\phi_{2^j} * I)(x,y) \end{aligned} \tag{3}$$

As we can see in (3) the two components of the wavelet transform of an image $I(x,y)$ at scale 2^j are equivalent to the gradient of the image smoothed by a corresponding scaling function ϕ_{2^j}.

The modulus of the wavelet transform is given by

$$d^{HV}_{2^j}(x,y) = \sqrt{|d^H_{2^j}(x,y)|^2 + |d^V_{2^j}(x,y)|^2} \tag{4}$$

and the angle of the wavelet transform vector is

$$A_{2^j}(x,y) = \tan^{-1}\left(\frac{d^V_{2^j}(x,y)}{d^H_{2^j}(x,y)}\right) \tag{5}$$

Shown in Fig.1(a) is an ultrasound image of the prostate, which is decomposed up to scale 2^4 via the wavelet transform. One of the most attractive characteristics of this transform is that the notable grey scale transitions within the original image, which correspond to the prominent features such as the prostate gland boundaries, are present as local maxima in the modulus of the wavelet decompostition, which are identified as bright pixels in Fig.1(b)-(c).

The transform provides us with the edge maps of the original image at different resolutions from the coarsest to the finest. Note the contours of the prostate are prominent in the coarser (large scale) edge maps. In contrast, the noise manifests itself in a random pattern and is mostly confined to the edge maps of small scales. This feature implies that we can obtain a rough boundary of the prostate from the edge map at the coarsest level to avoid the interference of the noise. Then we can refine the boundary by incorporating the information from the edge maps of lower scales. The angle of the two components of the wavelet transform also contains important information, which actaully gives us the orientation of the edge vector at each pixel. The angle at scale 2^4 is shown in Fig.1(d). The information of both the modulus and the angle will be employed later to locate the seed points, as described in the next subsection.

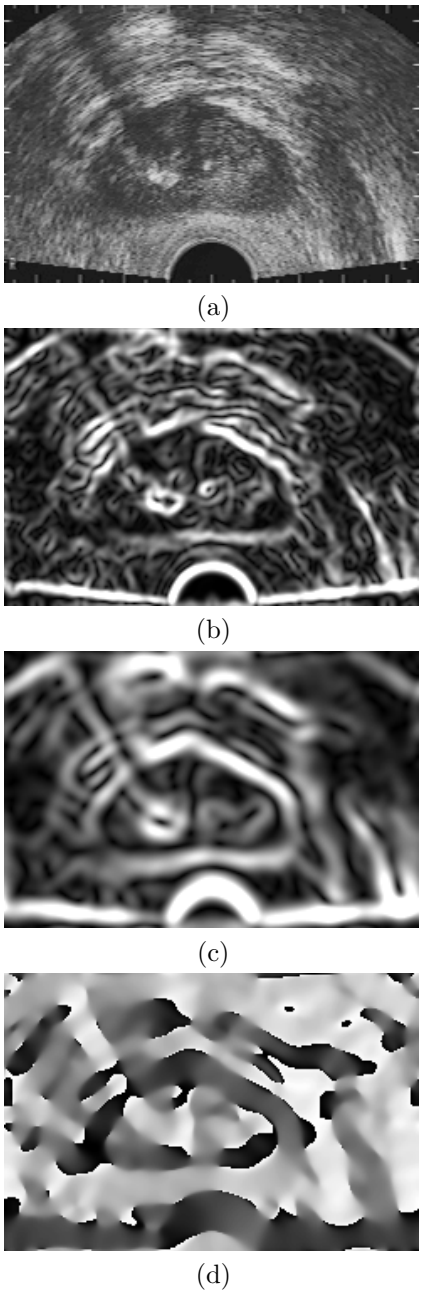

(a) (b) (c) (d)

Fig. 1. The wavelet decomposition of a prostate ultrasound image. (a) original image. (b) modulus $d^{HV}_{2^3}(x,y)$. (c) modulus $d^{HV}_{2^4}(x,y)$. (d) angle $A_{2^4}(x,y)$

B. Locating the Seed Points

The next step is to locate some preliminary boundary (seed) points in the coarsest edge map. First, an anchor point is set by the user, who also indicates the rough position of the first seed point. A number of radial lines are drawn from the anchor point and along these lines the radial profiles are extracted, as shown in Fig.2(a). Proceeding radially from the anchor point, a seed point is always characterised by a local maximum, which is larger than its two closest neighbours and strictly larger

than at least one of them.

As we can see in Fig.2(b) the boundary points are present as the local maxima along the radial profiles and the loci of the prostate contour are vaguely disernible. Most of the desired seed points are of large amplitude. However, some of them are very weak in strength resulting in broken segments. So it is necessary to find a strategy which somehow favours these points and finally claims them as seed points successfully. As we can see, every two adjacent desired seed points are close to each other because of the fact that the contour is relatively continuous. Apparently the next seed point should be sought within a small neighbourhood rather than "globally" along the radial profile.

Associated with each edge point is a tangent vector, which is perpendicular to the orientation of the edge vectors, that is, $A^t_{2^j}(x,y) = A_{2^j}(x,y) - \pi/2$. As we can see in Fig.2(c), the tangent vector of the previous seed point is roughly pointing to the position of next desired seed point. We also take the perpendicular line of the next radial line. The intersection points of these two lines with the next radial line defines a neighbourhood within which the next desired seed point will be sought. The points outside the neighbourhood are adversely weighted so that they will not challenge the local maximum within the neighbourhood, which is then asserted as the next seed point, as shown in Fig.2(d).

Fig.3 shows all the seed points successfully identified using this strategy. The plus sign indicates the anchor point and the cross is the first edge point, both selected by the user. These seed points will be used to initialise the snakes which are expected to find the contour eventually.

C. Snakes

A snake is a dynamic curve,

$$v(s) = (x(s), y(s)), \qquad s \in [0,1]$$

which moves within an image trying to minimize its energy, which is defined as the weighted sum of an internal energy and an external energy[5], [6].

$$\begin{aligned} E_{snake} &= \int_0^1 E_{int}(v) + \gamma E_{ext}(v) ds \\ &= \int_0^1 \frac{1}{2}\left(\alpha|v'(s)|^2 + \beta|v''(s)|^2\right) \\ &\quad + \gamma E_{ext}(v) ds \end{aligned} \tag{6}$$

The internal energy comes from within the curve itself and is defined as energy of continuity and energy of curvature. The external energy is usually set as the gradient of the image, which will draw the snake towards the salient features of the image, such as edges (high amplitude of gradient). The behaviour of the snake is controlled by the regularization parameters α, β, γ. A large α discourages stretching and makes the snake behave like an elastic string, which can shrink or contract. A snake with large β, which discourages bending and gives a dominant effect of smoothing, behaves more like a rigid rod. If we set β to zero, that is, switch off the influence of the bending effect, we can allow a sharp corner to form. The energy minimizing process can also be interpreted from a point of view of force balance. When the elastic force (corresponding to the energy of continuity), bending force (corresponding to the energy of curvature), and potential force (corresponding to the external energy) reach an equilibrium, the snake is expected to rest on the objects of interest within the image.

In our contour extraction scheme, the external energy is designated as the modulus of the wavelet transform, that is, $E_{ext}(v) = d^{HV}_{2^j}(v)$. The seed points obtained from the previous step are used to initialise a snake which evolves across the edge maps at different resolutions and finally stabilises and rests on the contour of the prostate, as shown in the next section.

III. Results

The seed points identified at scale 2^4 (Fig.3) are used to intialise a snake, which starts evolving from the edge map at scale 2^3 (Fig.1(b)). The control parameters are $\alpha = 0.2$, $\beta = 0.2$. γ is set to 1.1 to emphasize the image force at higher scales and reduced to 1.0 to make the snake immune to the interference from the noise. As we can see in Fig.4, the snake first contracts and smooths itself due to the influence of its internal energy. Gradually it is attracted to the prominent edges within the image due to the potential force. The stablised snake at scale 2^3 is then used to intialise a snake which will evolve within the edge map at scale 2^2 and directs itself towards finer feature within the edge map. The final contour found by the snakes is shown in Fig.5, which closely matches the edges disernible in the original image.

References

[1] F. Lee, S.T. Torp-Pedersen, D.B. Siders, P.J. Littrup, and R.D. McLeary, "Transrectal ultrasound in the diagnosis and staging of prostate carcinoma," *Radiology*, vol. 170, pp. 609–615, 1989.

[2] F. Lee, S.T. Torp-Pedersen, and R.D. McLeary, "Diagnosis of prostate cancer by transrectal ultrasound," *Urol. Clin. North Am.*, vol. 16, pp. 663–673, 1989.

[3] F. Zhao and C.J.S. deSilva, "Use of the Laplacian of Gaussian operator in prostate ultrasound image processing," *Proc. 20th Int. Conf. IEEE EMBS, Hong Kong*, vol. 2, pp. 812–815, 1998.

[4] S. Mallat and S. Zhong, "Characterization of signals from multi-scale edges," *IEEE Trans. Patt. Anal. Machine Intell.*, vol. 14, no. 7, pp. 710–732, July 1992.

[5] A. Witkin M. Kass and D. Terzopoulos, "Snakes: Active contour models," *Proc. 1st Int. Conf. Computer Vision, London, U.K.*, pp. 259–268, 1987.

[6] A. Witkin M. Kass and D. Terzopoulos, "Snakes: Active contour models," *Int'l. J. Computer Vision*, pp. 321–331, 1988.

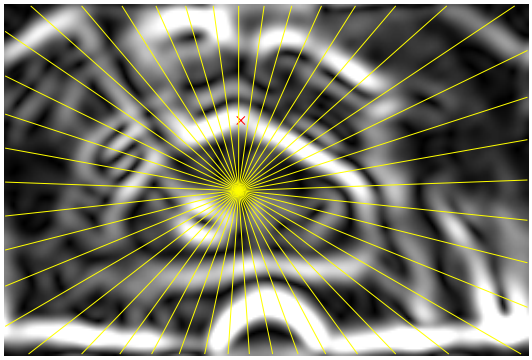

(a)

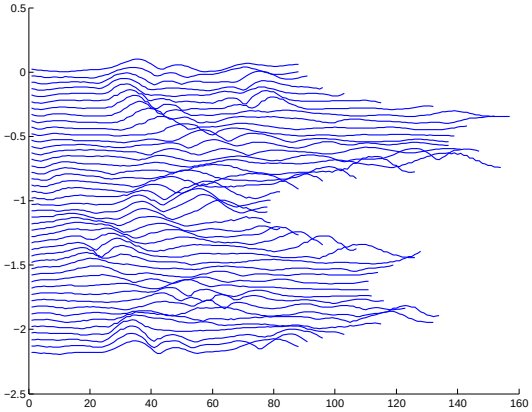

(b)

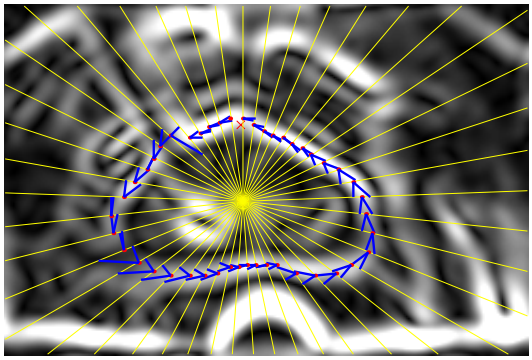

(c)

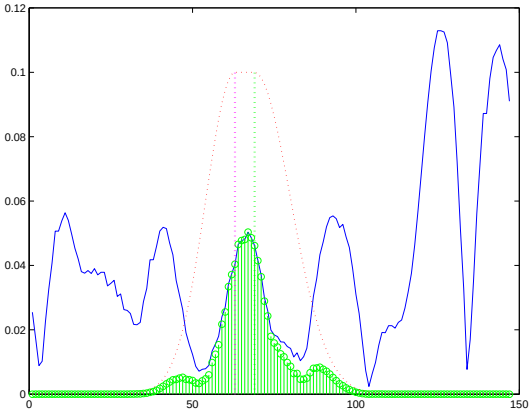

(d)

Fig. 2. Locating the seed points by maxima in radial profiles. (a) emanating radial lines. (b) radial profiles. (c) the tangent vectors and the perpendiculars. (d) locating the maximum.

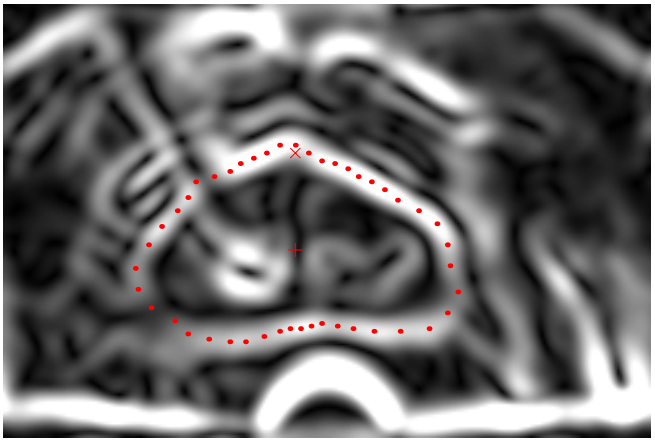

Fig. 3. Seed points identified at scale 2^4

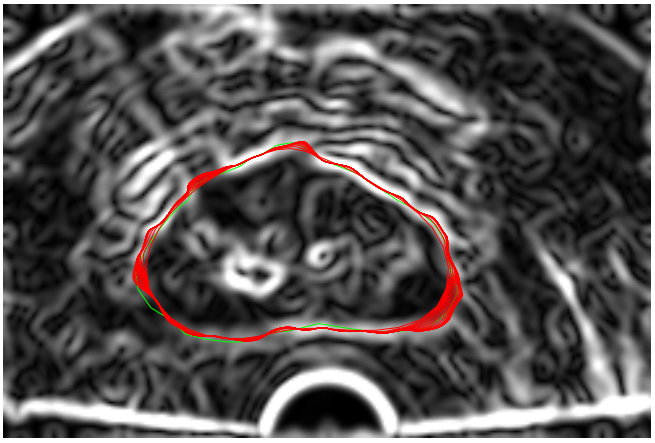

Fig. 4. Snake evolving at scale 2^3

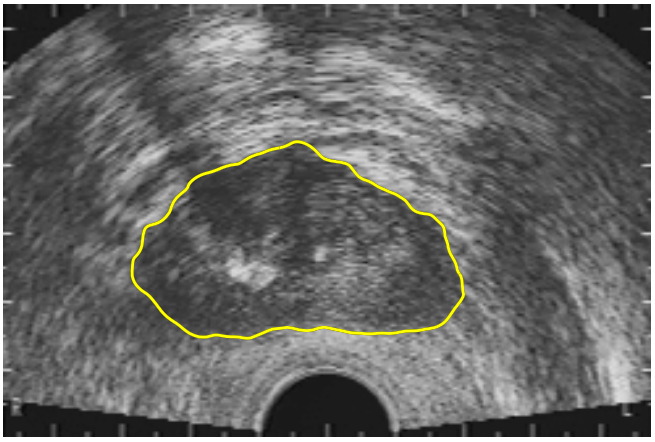

Fig. 5. Contour extracted